Packaging and system demonstration of an X-band phased array antenna utilizing highly dispersive photonic crystal fiber based true-time-delay

Harish Subbaraman*[a], Maggie Yihong Chen[b], Ray T. Chen[a]
[a]Microelectronic Research Center, Department of Electrical and Computer Engineering,
The University of Texas at Austin, Austin, Texas 78758, USA
[b]Omega Optics, Inc, 10435 Burnet Rd, Suite 108, Austin, TX 78758, USA

ABSTRACT

We demonstrate single RF beam transmission and reception of an X-band phased array antenna using highly dispersive photonic crystal fiber (PCF) based true-time-delay (TTD) lines. The dispersion coefficient of the fabricated fiber is as high as -600ps/nm/km at a wavelength of 1545nm. Coupling between a dispersion shifted fiber (DSF) and the fabricated PCF is performed by using an ultra high numerical aperture (UHNA) intermediate fiber, which helps in achieving a good coupling efficiency and keeping the insertion loss of the delay lines to under 3.5dB. Using the PCF-TTD network, we report the transmission of 8.4GHz signal at 7.4^0 and 12GHz signal at 21.2^0 by tuning the laser wavelength to 1547.72nm and 1552.52nm respectively. Single beam receiving capability is also demonstrated by accurately detecting 8.4GHz signal coming from -7.4^0 and 12GHz signal coming from -21.2^0 by tuning the wavelengths to 1547.72nm and 1552.52nm respectively..

Keywords: Dispersion, optical beamforming, phased-array antenna, photonic crystal fiber, true-time delay

1. INTRODUCTION

High performance phased-array antenna (PAA) system has been viewed as a key component in the military and civilian radar and communication systems. Much of the research focus has been on antenna and electronic phase-shifter development. However, traditional electrical feeding networks have an intrinsic narrow band nature. Various optical schemes have been proposed and demonstrated to take advantage of a photonic feed for true-time delay (TTD) including acousto-optic integrated circuit technique [1], Fourier optical technique [2], bulky optics techniques [3], dispersive fiber technique [4–9], fiber grating technique [10, 11], and substrate-guided wave technique [12]. Optical true-time-delay (TTD) provides a broad bandwidth and squint-free operation apart from advantages such as EMI-free operation, small size, light weight etc. Esman et al. proposed a fiber-optic TTD technique using conventional dispersion compensating fiber (DCF) to meet these requirements [5]. However, the dispersion parameter, D, of conventional DCF is small ($D \approx -100$ ps/nm·km), and therefore long fiber lengths are still needed in the TTD module to get the required time delay. By using a fiber with a very high dispersion coefficient, it is possible to reduce the size and weight of the system significantly.

The four element true-time-delay network consists of different lengths of highly dispersive photonic crystal fiber (PCF) with a very high dispersion coefficient of ~ -600ps/nm/km at a wavelength of 1550nm connected to different lengths of dispersion shifted fibers (DSF) in each arm [13, 14]. The longest length of PCF used in the lines is equal to 10.5m. In order to achieve good coupling efficiency between the PCF and DSF is obtained by using a short length an ultra high numerical aperture (UHNA) intermediate fiber between the PCF and the DSF. The TTD network is characterized to provide continuous delay from -28.3ps to 31.3ps by tuning the optical wavelength from 1530nm to 1560nm, which is sufficient to scan from -41^0 to 45^0 for a 4-element PAA subarray having 1.3cm element spacing. Since the dispersion coefficient of the fabricated photonic crystal fibers is greater than that of a telecom SMF-28 fiber, which has a dispersion coefficient of 18ps/nm/km, the length of the delay line can be reduced by the same factor.

Photonics Packaging, Integration, and Interconnects IX, edited by Alexei L. Glebov, Ray T. Chen,
Proc. of SPIE Vol. 7221, 722107 · © 2009 SPIE · CCC code: 0277-786X/09/$18 · doi: 10.1117/12.811027

2. HIGHLY DISPERSIVE PHOTONIC CRYSTAL FIBER

2.1 A. Working Principle

The photonic crystal fiber (PCF) was first demonstrated by Knight et al in the year 1996 [15]. A PCF consists of a periodic cladding made up of an array of air holes running down the entire length of the fiber. Due to the presence of such a cladding, PCF provides excellent flexibility in controlling the characteristics of the fiber such as nonlinearity, dispersion etc by controlling the structural parameters of the fiber. The PCF is usually fabricated using stack and draw technique. For our application, a high dispersion is of interest. One of the structures that can lead to very high dispersion coefficients is based on a dual concentric-core design [16]. The mechanism of a dual concentric-core PCF is very similar to that of a directional coupler. First, we introduce the coupled mode theory on the dual core PCFs [11]. The central core and the outer core behave like two parallel waveguides and the high dispersion is from the coupling between the two waveguides. By expanding the propagation constants, β, of the modes in the isolated waveguides around the phase matched frequency using Taylor's series, we get [16]

$$\beta_i(\omega) \approx \beta(\omega_p) + (\omega-\omega_p)\frac{d\beta_i}{d\omega}\bigg|_{\omega=\omega_p} + \frac{(\omega-\omega_p)^2}{2}\frac{d^2\beta_i}{d\omega^2}\bigg|_{\omega=\omega_p} \tag{1}$$

where i = 1, 2 represents the inner and the outer waveguide respectively and ω_p represents the phase matched frequency. From the coupled mode theory, we know that the coupling of the individual modes can generate two super-modes, whose propagation constants can be written as [16]

$$\mathrm{B}_{+/-} = \frac{1}{2}\{[\beta_1(\omega)+\beta_2(\omega)] \pm \sqrt{[\beta_1(\omega)-\beta_2(\omega)]^2 + 4\kappa^2}\} \tag{2}$$

where κ is the coupling constant between the two waveguides. We can insert Eq. (1) into Eq. (2) and differentiate the result twice with respect to angular frequency. Supposing that the two waveguides' $\frac{d^2\beta}{d\omega^2}\Big|_{\omega=\omega_p}$ are all very small numbers (this term is mainly determined by the material dispersion of waveguide, and so it must be a very small term), we get the group velocity dispersion as

$$\frac{d^2\mathrm{B}_{+/-}}{d\omega^2} = \pm\frac{1}{4\kappa}\left(\frac{d\beta_1}{d\omega}-\frac{d\beta_2}{d\omega}\right)^2 \times \left[\frac{(\omega-\omega_p)^2}{4\kappa^2}\left(\frac{d\beta_1}{d\omega}-\frac{d\beta_2}{d\omega}\right)^2+1\right]^{-\frac{3}{2}} \tag{3}$$

The dispersion parameter is defined as

$$D = -\frac{\lambda}{c}\frac{d^2 n_{eff}}{d\lambda^2} = -\frac{2\pi c}{\lambda^2}\frac{d^2 B}{d\omega^2} \tag{4}$$

Using Eq. (3) and Eq. (4) we get,

$$D = \mp\frac{\pi}{2c\kappa}\left(\frac{dn_1}{d\lambda}-\frac{dn_2}{d\lambda}\right)^2 \times \left[\frac{\pi^2}{\kappa^2}\frac{(\lambda-\lambda_p)^2}{\lambda_p^2}\left(\frac{dn_1}{d\lambda}-\frac{dn_2}{d\lambda}\right)^2+1\right]^{-3/2} \tag{5}$$

From Eq. (5), we see that the dispersion value reaches its maximum value when λ is equal to λ_p and is given by

$$D_{Max} = \mp\frac{\pi}{2c\kappa}\left(\frac{dn_1}{d\lambda}-\frac{dn_2}{d\lambda}\right)^2 \tag{6}$$

From Eq. (6), we see that the dispersion value mainly depends on the coupling constant κ and the difference of $dn/d\lambda$ between the inner and the outer core. The parameters of the fiber were carefully chosen to make the respective

modes have a phase match at a wavelength (λ_P) close to 1.55 μm. At the phase match wavelength around 1.55 μm, the effect of varying the period (Λ) on dn/dλ and coupling constant κ are carefully studied using fully vectorial plane wave expansion (PWE) method [17]. Since the PCF is not a perfect crystal without defects, a supercell of size 10 x 10, instead of a unit cell is implemented for periodic boundary conditions. From simulations we find that the period (Λ) plays a vital role in achieving broadband operation along with a very high dispersion value. By designing structures with very small periods, we can achieve very high dispersion-bandwidth products. However, it becomes very difficult to control the diameter of the air holes over such small dimensions. Simulations also show that any small deviation in the air hole diameters can totally change the dispersion curve in terms of magnitude and position. Therefore, the parameters need to be strictly controlled while drawing the fibers. This sets a limit on the manufacturability. Higher dispersion value requires smaller inner core diameter (~ 1.5 μm), which makes the coupling from a standard single mode fiber to this fiber very difficult and lossy.

2.2 True Time Delay (TTD) network using highly dispersive PCF:

The SEM and the schematic cross section of a practical high dispersion PCF are shown in Fig. 1(a) and 1(b) respectively [B67]. The PCF has a pitch (□) = 3.5 μm, d_0 = 1.72 μm, d_1 = 1.45 μm, d_2 = 1.08 μm, d_3 = 0.86 μm. The inner core doping is 1.9% and the outer core doping is 1.2%. The fiber was fabricated by Crystal Fibre A/S, Denmark.

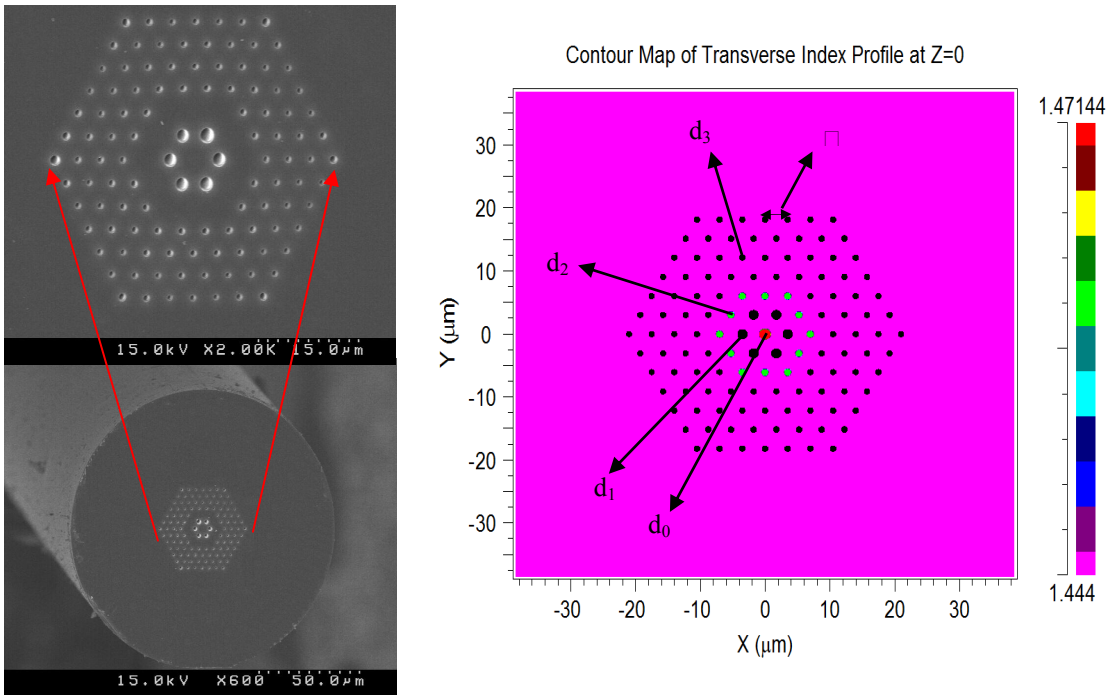

(a) (b)

Fig. 1(a) Scanning electron microscope (SEM) images of the fabricated high dispersion PCF [B67], (b) Schematic cross section of the PCF.

Using the highly dispersive PCF, a four element true-time-delay network is formed. The first element is made up of 10.5m DSF; the second element consists of 3.5m of DSF and 7.0m PCF; the third element consists of 7.0m of DSF and 3.0m of PCF; the fourth element consists of 10.5m PCF. In order to measure the dispersion coefficient of the fiber, at each wavelength (λ) time delay (in ps) is measured using a network analyzer at (λ+0.1nm) and (λ-0.1nm). The difference of time delay between (λ+0.1nm) and (λ-0.1nm) divided by 0.2nm divided by the length of the PCF in km gives the dispersion coefficient. The measured dispersion coefficient as a function of wavelength is shown in Fig. 2. The figure also shows the computed steering angle for an antenna array with inter-element spacing = 1.3cm.

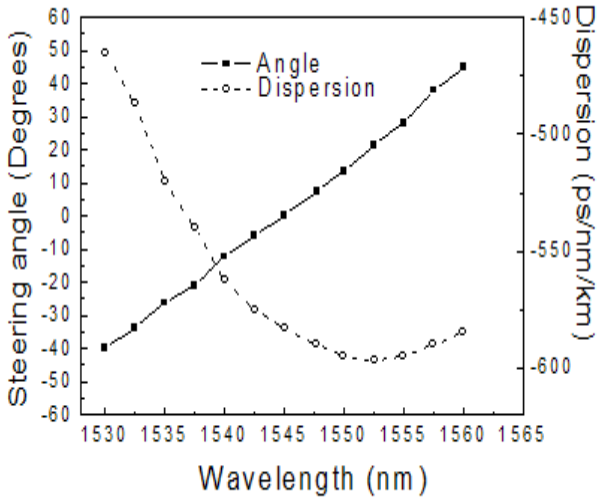

Fig. 2. Measured dispersion coefficient of the PCF as a function of wavelength (dashed curve). Calculated beam steering angle (solid curve) is also shown for an antenna array with inter-element spacing = 1.3cm.

It can be seen from the above figure that the dispersion coefficient is as large as -600ps/nm/km. This value is 33 times larger compared to the dispersion coefficient of conventional single mode fibers, and about 6 times greater than dispersion compensation fibers. Therefore, the length of the TTD line can be reduced by the same factors.

Usually, there is a mode field diameter mismatch between the DSF and the PCF. Therefore, a very short length of ultra high numerical aperture (UHNA) fiber is spliced between the DSF and the PCF. A schematic representation of the connection between the PCF and DSF using UHNA fiber is shown in Fig. 3.

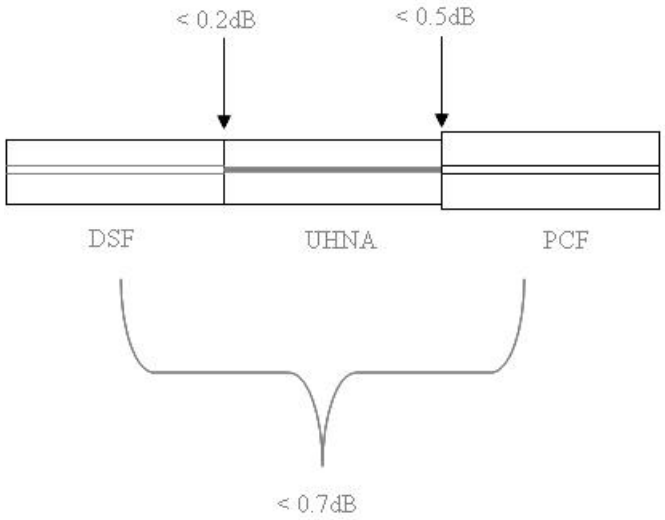

Fig. 3. Schematic representation of connection between DSF and PCF using UHNA fiber.

The splices are protected with splice sleeves. Using such a connection, the largest insertion loss of the 4 delay lines is less than 3.5dB.

2.3 Phase versus Frequency measurement:

In order to show the TTD nature of the highly dispersive PCF and also to measure the time delay, a phase versus frequency measurement is necessary. For this purpose, a network analyzer (HP8510C) is used. The schematic of the setup is shown in Fig. 4. The RF signal from the network analyzer is modulated onto an optical carrier generated by the tunable laser source using a Lithium Niobate Mach-Zehnder Modulator (MZM). The modulated carrier is split into two channels using a 1-to-2 splitter. One output arm of the splitter feeds the reference TTD line (10.5m DSF in this case) and the other output arm is fed to the TTD line under test. The phase of the output signal is measured with respect to the reference arm on the network analyzer.

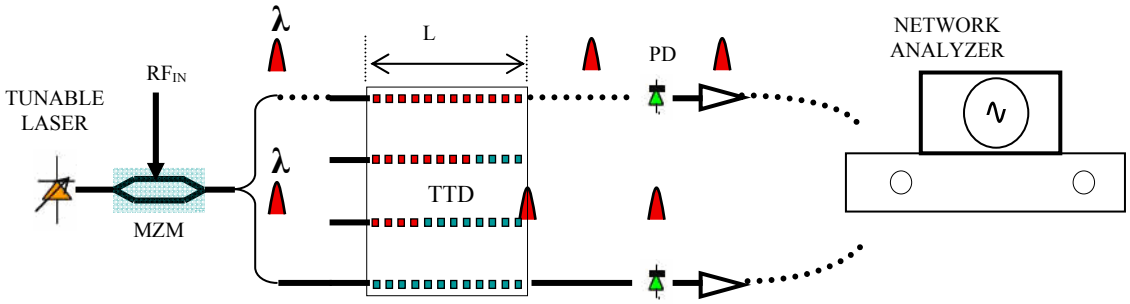

Fig. 4: Schematic of Phase versus Frequency measurement setup.

The RF signal is changed from 8GHz to 12GHz. This procedure is repeated at a different wavelength by tuning the laser wavelength. The measured phase versus frequency curves for the TTD lines are shown in Fig. 5. It can be seen from the figure that the phase vs. frequency plots are straight lines. This is a characteristic of true time delay networks. Also, the slope of the lines gives the time delay value. By changing the wavelength from 1530nm to 1560nm, a continuous time delay between -28.3ps to 31.3ps can be achieved. This translates to a steering angle of -41^0 to 46^0 for an X band antenna array with inter-element spacing = 1.3cm.

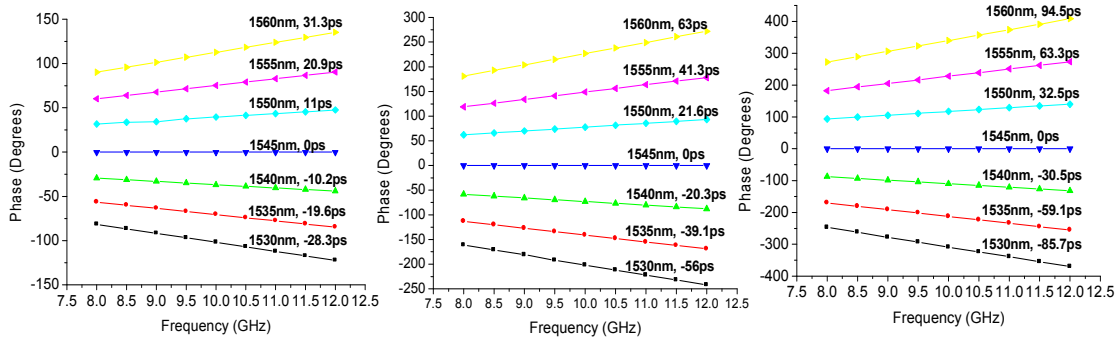

(a) (b) (c)

Fig. 5. Phase versus Frequency plots. (a) TTD lines consists of 3.5m PCF and 7.0m DSF, (b) TTD line consists of 7.0m PCF and 3.5m DSF, (c) TTD line consists of 10.5m PCF and 0m DSF

Since the DSF sections are trimmed for all the TTD lines to have the same delay value at 1545nm, the phase versus frequency plot is a straight line with slope = 0 for all the lines. It can also be seen from the figure that at a particular wavelength, there is a near-constant time delay between adjacent elements. At a different wavelength, the constant is different. Therefore, by tuning the wavelength, the beam can be steered continuously.

3. SINGLE RF BEAM TRANSMISSION

The actual experimental setup used for the demonstration of dual beam steering is shown in Fig. 6. Optical carrier from an external cavity tunable laser source is modulated with an RF signal generated by HP 8510C network analyzer, using a high speed $LiNbO_3$ modulator. The modulated optical signal is amplified using an Erbium-doped fiber amplifier (EDFA). The amplified signal is split into 4 channels using a 1:4 optical power splitter and distributed to the four TTD lines shown in Fig. 6(b). The total length L, of each delay line is 10.5 meters, and the lengths of PCF segments used in the 4 delay lines are 0m, 3.5m, 7m, and 10.5m respectively. The lengths are chosen such that at a wavelength of 1545nm, the nominal delay through each TTD line is the same. This implies that at 1545nm, the RF signal is radiated broadside at the X-band (8-12GHz) antenna array. The photodetector bank converts the optical signals into electrical signals, which are then amplified by the X-band low noise amplifiers (LNA). After amplification, the electrical signals are fed to a 4-element X-band antenna array, which has an element spacing of 1.3cm. The radiated power is received by a horn antenna and the received power is measured using a microwave spectrum analyzer (MSA) shown in Fig. 6(c).

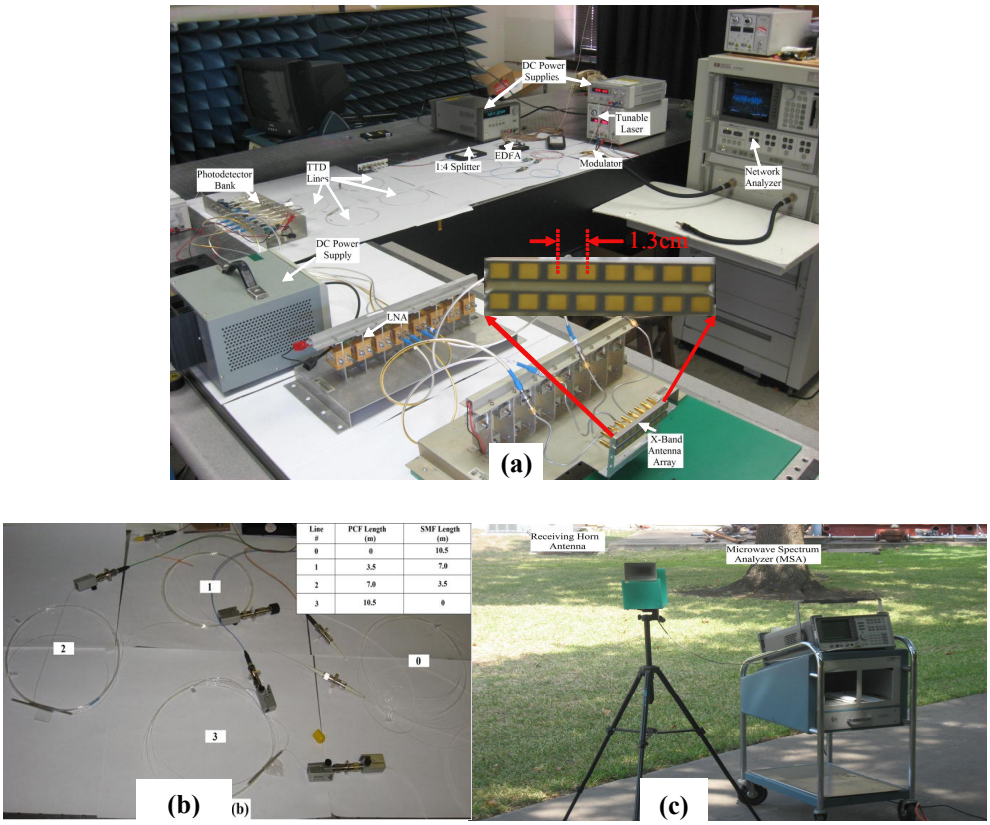

Fig. 6. Experimental setup of the PAA in transmitting mode. (a) Overall setup along with an expanded view of the antenna array is shown. EDFA: Erbium-Doped Fiber Amplifier; TTD: true-time-delay; LNA: low noise amplifier (b) The four TTD lines are shown. The inset shows the composition of each line. (c) The receiving horn antenna and the microwave spectrum analyzer for measuring received power.

The far field radiation pattern is measured by fixing the PAA on an accurate positioner and measuring the received power at a fixed standard horn antenna connected to a microwave spectrum analyzer (MSA). The measured steering angle of an 8.4GHz signal is 7.4^0 at a wavelength of 1547.72nm, and is 21.2^0 for a 12GHz signal at 1552.52nm as shown in Fig. 7. It can be seen from Figs 7(a) and 7(b) that the measured patterns agree well with the simulated results, showing the capability of single beam transmitting capability of the system

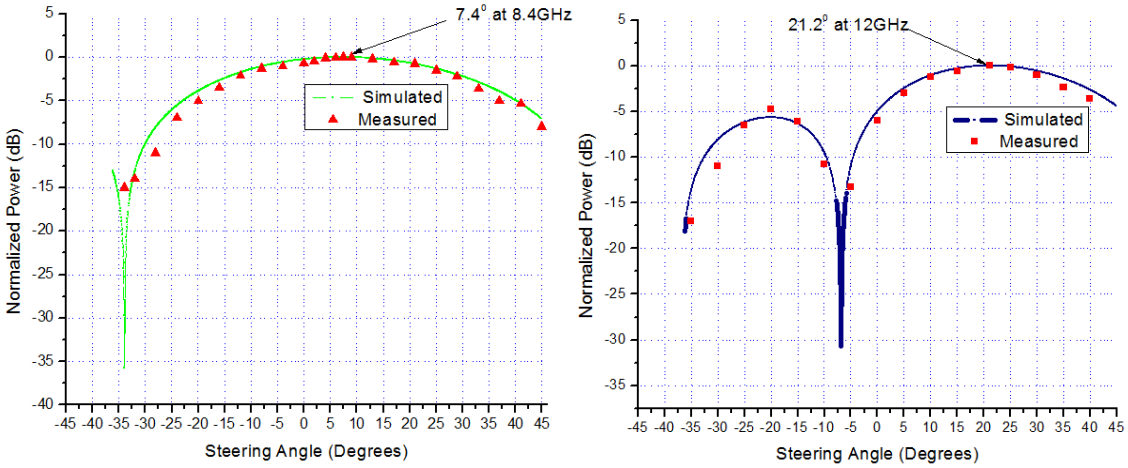

(a) (b)

Fig. 7. Simulated and measured far field patterns (a) RF signal with frequency = 8.4GHz is steered to 7.4^0 using a wavelength of 1547.72nm. (b) RF signal with frequency = 12GHz is steered to 21.2^0 using a wavelength of 1552.72nm.

4. SINGLE RF BEAM RECEPTION

In the previous section, experimental results for single RF beam transmission were presented. In this section, the operation of the PAA is extended to receive and accurately determine the angle of arrival of the incoming beam. The schematic of the setup used for the receiving mode of the PAA is shown in Fig. 8.

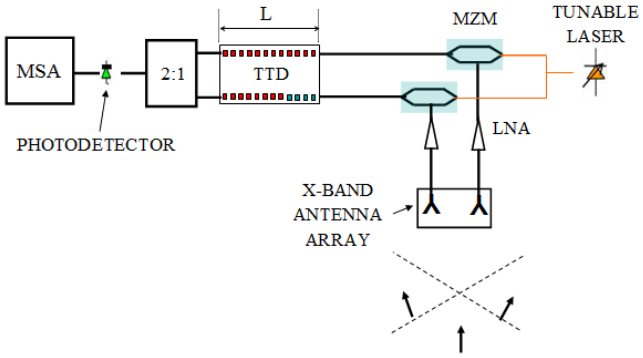

Fig. 8. Schematic of the PAA setup for single beam reception. LNA: low noise amplifier; MZM: Mach-Zehnder modulator; TTD: true-time-delay; MSA: microwave spectrum analyzer

In the case of transmitting mode, only one modulator is required to modulate the RF signal onto the optical carrier. In the case of receiving mode however, since each element receives the RF signal, one modulator per antenna element is required. Since we are limited by the hardware, the receiving mode experiment is performed using two antenna elements. Only minor modifications to the transmitting mode experiment needs to be made in order to set the experiment up in the receiving mode.

Since the incoming beam travels a different path length in order to reach each element, a phase difference between the two signals is created. The RF signals from the antenna elements are amplified and modulated onto the optical carrier. The TTD lines also induce additional phase shifts. Therefore, if the additional phase shift has a sign opposite to the once created by the incoming beams, then the two signal coming out of the TTD lines will be in phase and they will add up to give a maximum. Thus, if the incoming beam is arriving from a direction 'θ', then the optical wavelength that can cancel the phase difference is the one that would direct a beam at an angle of '-θ' in the transmitting mode. Therefore, there is a peak on the plot of the combined power at the photodetector versus wavelength. The wavelength at which the peak

occurs can be used in conjunction with steering angle data as shown in Fig. 2 can be used to determine the angle of arrival.

In order for the receiving mode experiment results to be consistent with transmitting mode experiment results, the incoming RF beams are chosen to have frequencies of 8.4GHz and 12GHz. The 8.4GHz signal impinges on the array from an angle of -7.4^0. As the wavelength is scanned, a peak in the power at the photodetector is measured at a wavelength of 1547.72nm as shown in Fig. 9(a). This corresponds to a complementary angle of 7.4^0 in the transmitting mode. Similary, fig. 9(b) shows the results for 12GHz signal source placed at -21.2^0. It can be seen that the peak occurs at 1552.52nm, which corresponds to a complementary angle of 21.2^0 in the transmitting mode. These results show the feasibility of using the PCF TTD based X-Band PAA in the receiving mode.

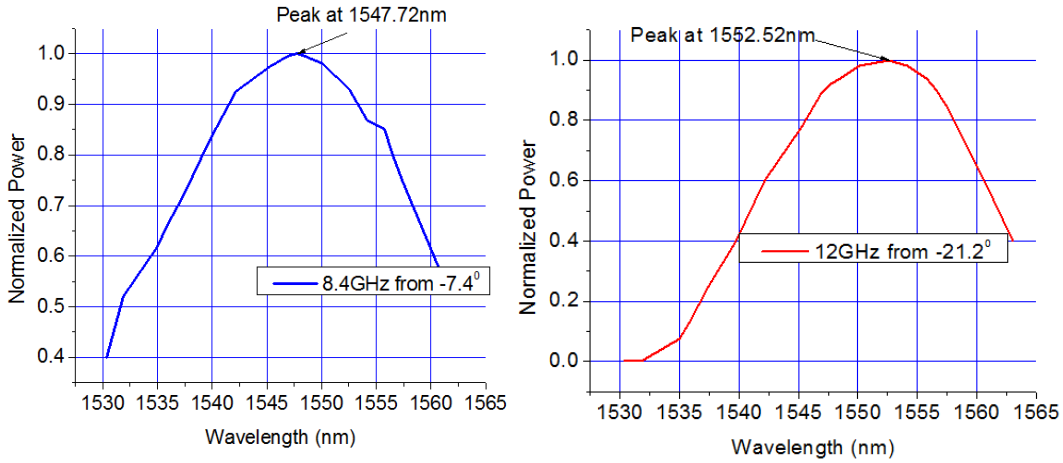

Fig. 9. Measured received power versus wavelength. (a) A peak at 1547.72nm occurs for an RF signal with frequency 8.4GHz arriving from -7.4^0. (b) A peak at 1552.52nm occurs for an RF signal with frequency 12GHz arriving from -21.2^0.

5. CONCLUSIONS

We have formed a True-Time-Delay network utilizing highly dispersive photonic crystal fibers. The mode field diameter mismatch between the PCF and DSF is addressed using an ultra high numerical aperture intermediate fiber. The TTD network is used to demonstrate single RF beam transmission and receiving capability. Using such a small size, low weight architecture, RF beam can be continuously steered from -41^0 to $+46^0$ by tuning the wavelength of the optical carrier from 1530nm to 1560nm.

REFERENCES

[1] L. H. Gesell, R. E. Feinleib, J. L. Lafuse, and T. M. Turpin, "Acousto-optic control of time delays for array beam steering," Proc. SPIE 2155, 194–204 (1994).

[2] G. A. Koepf, "Optical processor for phased-array antenna beam formation," Proc. SPIE 477, 75–81 (1984).

[3] N. A. Riza, "Liquid crystal-based optical time delay units for phased array antennas," J. Lightwave Technol. 12, 1440–1447 (1994).

[4] R. Soref, "Optical dispersion technique for time-delay beam steering," Appl. Opt. 31, 7395–7397 (1992).

[5] R. D. Esman,., "Fiber-optic prism true time-delay antenna feed," *IEEE Photonics Technology Letters*, vol. 11, 1993, pp. 1347-1349.

[6] R. D. Esman, M. J. Monsma, J. L. Dexter, and D. G. Cooper, "Microwave true time-delay modulator using fibre-optic dispersion," Electron. Lett. 8, 1905–1907 (1992).

[7] R. D. Esman and L. Goldberg, "Fiber optic true time delay array antenna feed system," U.S. patent 6,337,660 (January 8, 2002).

[8] M. Y. Frankel, P. J. Matthews, and R. D. Esman, "Fiber optic true time steering of an ultrawideband receive array," IEEE Trans. Microwave Theory Tech. 45, 1522–1526 (1997).
[9] M. Y. Frankel, R. D. Esman, and M. G. Parent, "Phased-array transmitter/receiver controlled by a true time-delay fiber optic beamformer," IEEE Photonics Technol. Lett. 7, 1216–1218 (1995).
[10] A. Moloney, C. Edge, and I. Bennion, "Fiber grating time delay elements for phased array antennas," Electron. Lett. 31, 1485–1486 (1995).
[11] J. E. Roman, M. Y. Frankel, P. J. Matthews, and R. D. Esman, "Time-steered array with a chirped grating beamformer," Electron. Lett. 33, 652–653 (1997).
[12] Y. Chen and R. T. Chen, "A fully packaged true time delay module for a K-band phased array antenna system demonstration," IEEE Photonics Technol. Lett. 14, 1175–1177 (2002).
[13] Y. Jiang, B. Howley, Z. Shi, Q. Zhou, R. T. Chen, M. Y. Chen, G. Brost, and C. Lee, "Dispersion-Enhanced Photonic Crystal Fiber Array for a True Time-Delay Structure X-band Phased Array Antenna," IEEE. Photon. Technol. Letts. **17**, 187-189 (2005).
[14] Y. Jiang, Z. Shi, B. Howley, X. Chen, M. Y. Chen, and R. T. Chen, "Delay Time Enhanced Photonic Crystal Fiber array for Wireless Communications using 2-D X-band Phased-Array Antennas," Opt. Engineering. **44**, 125001 (2005).
[15] J. C. Knight, T. A. Birks, P. St. J. Russell, and D. M. Atkin, "All-silica single-mode optical fiber with photonic crystal cladding," Optics Letters, Vol. 21, 1547-1549 (1996)
[16] U. Peschel, T. Peschel, and F. Lederer, "A compact device for highly efficient dispersion compensation in fiber transmission," Appl. Phys. Lett. 67, 2111-2113 (1995).
[17] K. M. Ho, C. T. Chan, C. M. Soukoulis, "Existence of a Photonic Gap in Periodic Dielectric Structures," Phy. Rev. Lett. 65, 3152-3155 (1990).